

Figures Calculus III

Felix Claeys, Brecht Verbeken, Simon Verbruggen

October 10, 2025

1.2.3 Example evolute cycloid

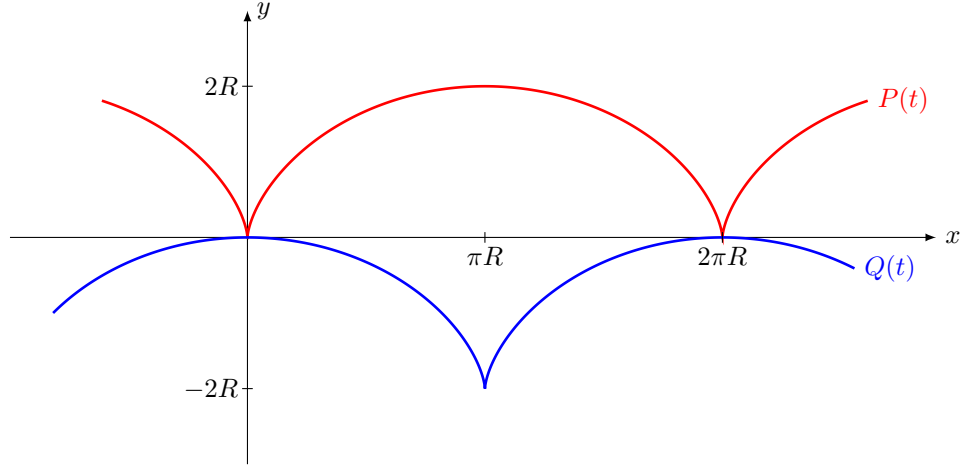


Figure 1: The cycloid $P(t) = [R(t - \sin t), R(1 - \cos t)]$ and its evolute $Q(t) = [R(t + \sin t), R(\cos t - 1)]$, which is a translation of $P(t)$.

1.2.4 Example evolute catenary

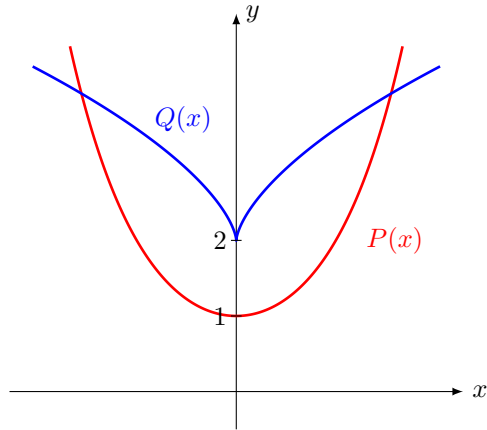


Figure 2: The catenary $P(x) = [x, a \cosh(x/a)]$ and its evolute $Q(x) = [x - \frac{a}{2} \sinh(2x/a), 2a \cosh(x/a)]$.

1.2.5 Example involute catenary (tractrix)

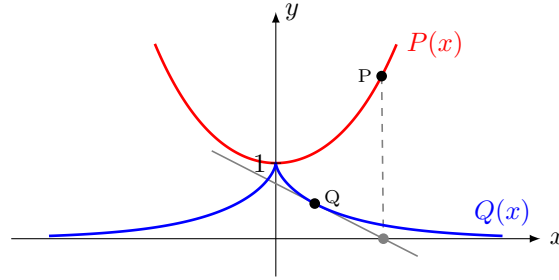


Figure 3: The catenary $P(x) = [x, a \cosh(x/a)]$ and its involute: the tractrix $Q(x) = [x - a \tanh(x/a), \frac{a}{\cosh(x/a)}]$. For a point Q on the tractrix, the intersection of the tangent to Q with the X -axis coincides with the orthogonal projection of the corresponding point on the catenary P .

1.2.8 Example envelope family of straight lines

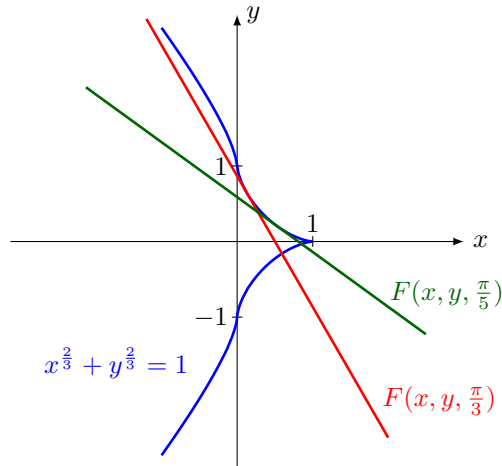


Figure 4: Some examples from the family of lines $F(x, y, a) = \frac{x}{\cos(a)} + \frac{y}{\sin(a)} = 1$, and the corresponding astroid: $x^{2/3} + y^{2/3} = 1$.

2.3 Gradient of scalar field

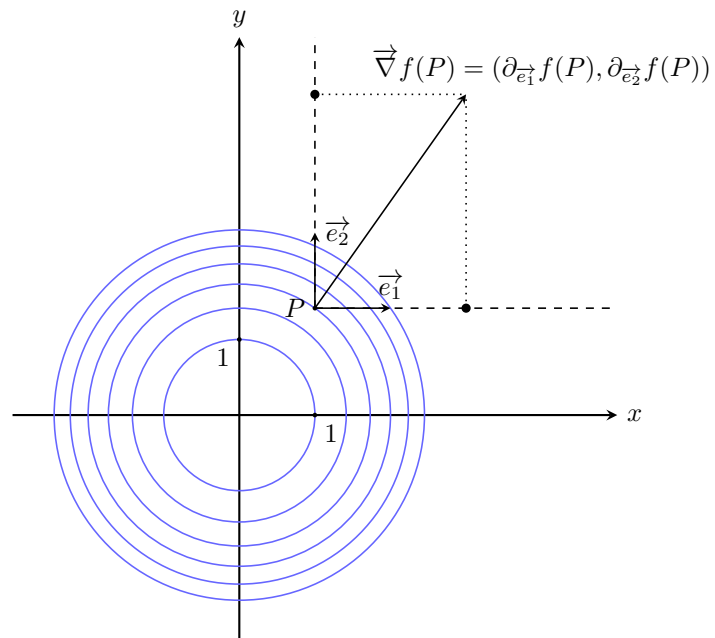


Figure 5:

3.1 Line integral of a scalar field

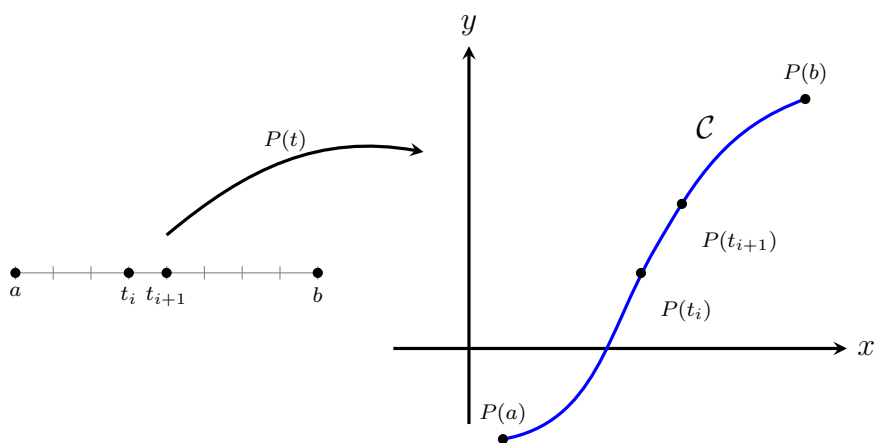


Figure 6: The line integral of a scalar field ϕ over a smooth curve $P(t)$ is given by: $\int_{\mathcal{C}} \phi \, ds := \int_a^b \phi(P(t)) \left\| \frac{d\vec{P}}{dt} \right\| dt$. In the figure, the displacement between different points along the curve, $P(t_{i+1}) - P(t_i)$, is shown. This relates to the infinitesimal displacement $\left\| \frac{d\vec{P}}{dt} \right\| dt$.

3.2 Line integral of a vector field

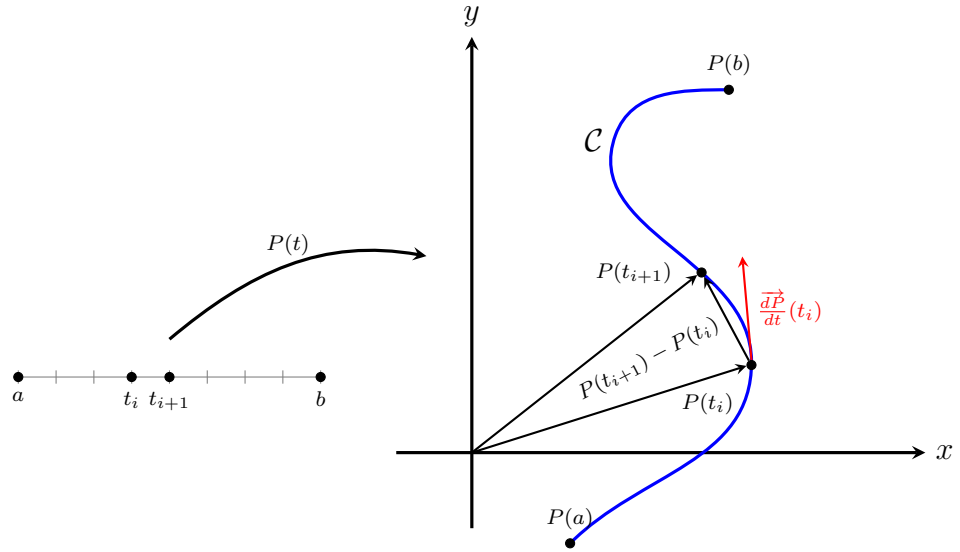


Figure 7: The line integral of a vector field \vec{F} over a smooth curve $P(t)$ is given by: $\int_C \vec{F} \cdot d\vec{P} := \int_a^b \vec{F}(P(t)) \cdot \frac{d\vec{P}}{dt} dt$. In the figure, the displacement between different points along the curve, $P(t_{i+1}) - P(t_i)$, is shown. This relates to the infinitesimal displacement vector $\frac{d\vec{P}}{dt} dt$.

3.4.2 Conservative field along a curve

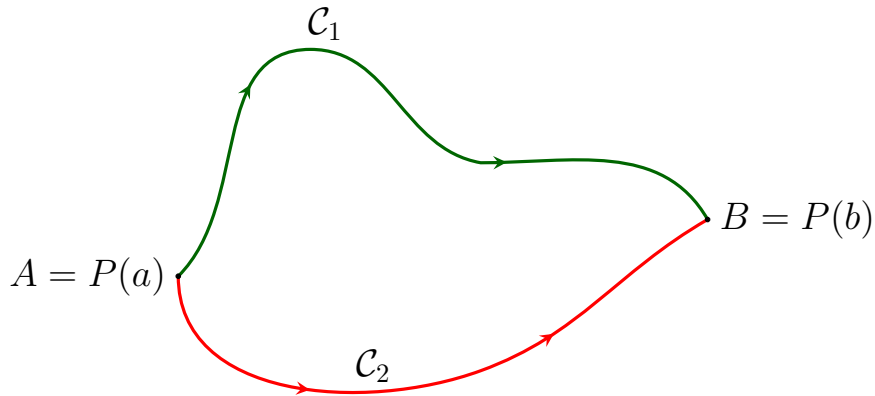


Figure 8: The points A and B lie on a closed curve \mathcal{C} . We can choose two arbitrary paths, \mathcal{C}_1 and \mathcal{C}_2 , from A to B . If we evaluate the line integral of a conservative field ϕ along both paths, the result will be the same, since the line integral of a conservative field is independent of the travelled path.

3.4.3 Proof conservative field

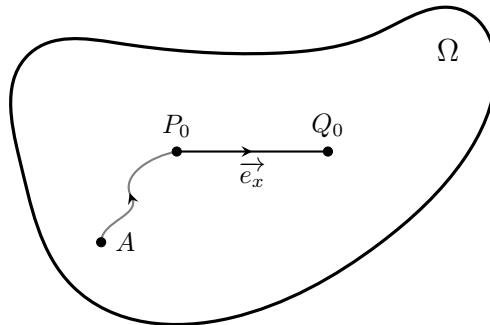


Figure 9: Proof that path-independence implies conservativeness in fields. Consider a path-independent vector field \vec{F} in an open, connected region Ω . A potential function $\phi(P_0)$ is constructed by integrating \vec{F} along an arbitrary curve $\widehat{AP_0}$ from a fixed point A to P_0 . The path independence ensures that ϕ is well-defined, and its gradient reproduces \vec{F} .

3.5.1 Proof Greens theorem

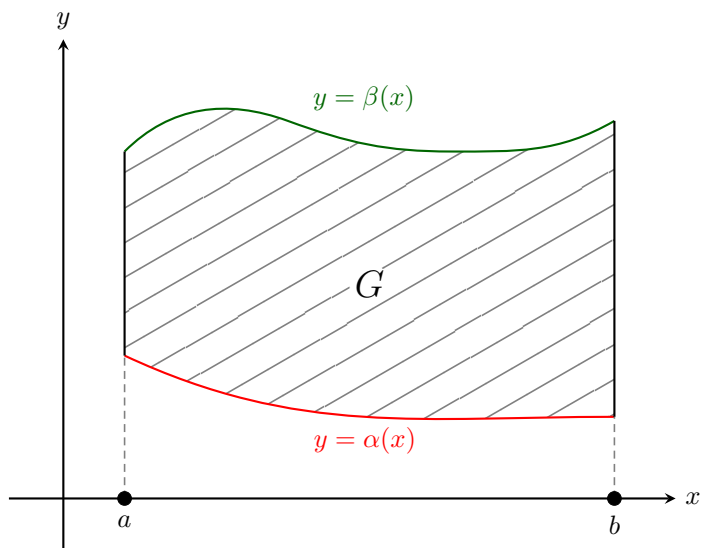


Figure 10: The normal region G can be projected onto the x -axis, with its upper and lower boundaries parametrized by $y = \alpha(x)$ and $y = \beta(x)$.

3.5.2 Union of normal spaces

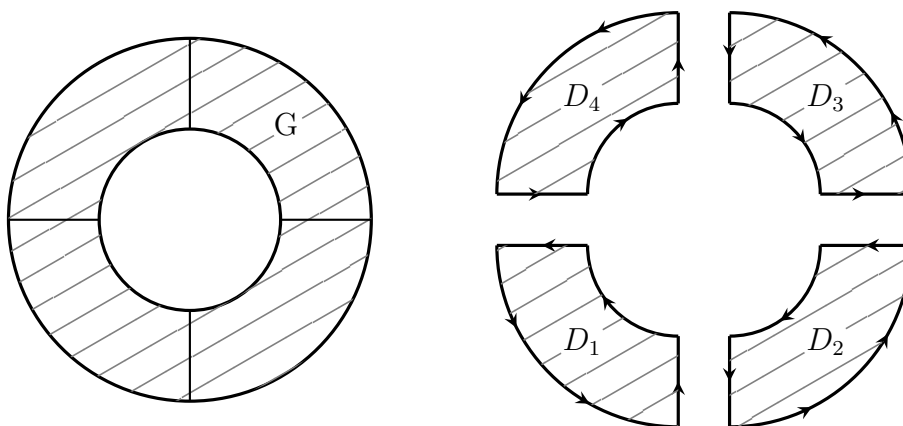


Figure 11: (Left) The annulus G is not a normal region, as it cannot be projected onto the X - or Y -axis. (Right) However, G is a union of normal regions: it can be split into four regions (D_i) each of which can be projected onto the X - and Y -axis.

3.5.4 Alternative formulation Greens theorem

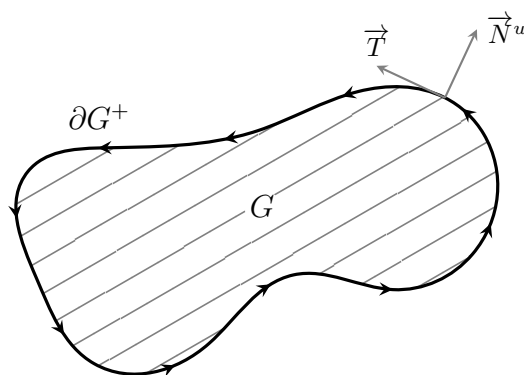


Figure 12: The alternative representation of Green's theorem: $\int_{\partial G^+} \vec{F} \cdot \vec{N}^u ds = \int_G \vec{\nabla} \cdot \vec{F} dA$, where \vec{T} is the tangent unit vector and \vec{N}^u the outward normal vector.

4.1 Surface integral of a scalar field

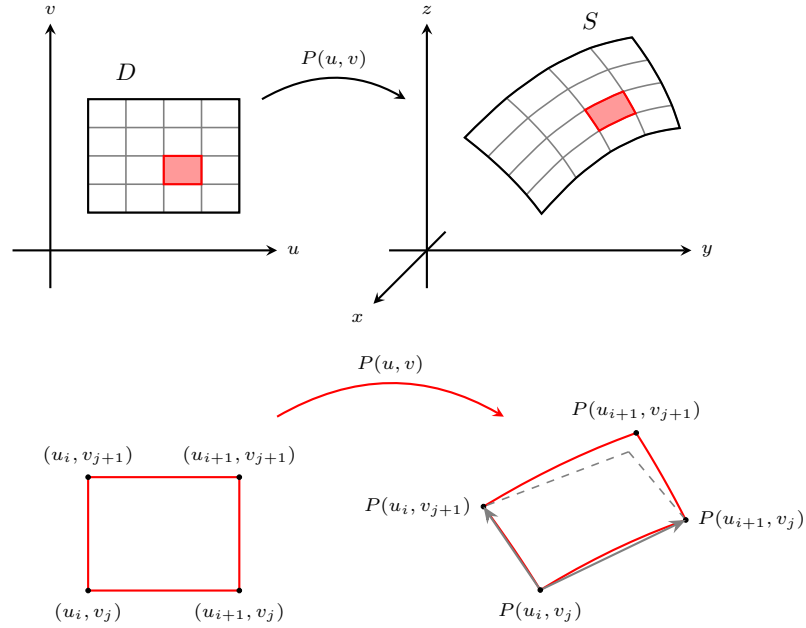


Figure 13: Construction of the surface integral of a scalar field ϕ over a smooth surface $S = P(u, v)$: $\int_S \phi \, d\sigma := \int_D \phi(P(u, v)) \|\overrightarrow{\partial_u P} \times \overrightarrow{\partial_v P}\| \, du \, dv$ (Below) An infinitesimal rectangle on D with area $du_i \, dv_j$ is projected onto a curvilinear quadrilateral on S , which we can approximate by a parallelogram, with area: $|(P(u_{i+1}, v_j) - P(u_i, v_j))(P(u_i, v_{j+1}) - P(u_i, v_j))| = \|\overrightarrow{\partial_u P(u_i, v_j)} \times \overrightarrow{\partial_v P(u_i, v_j)}\| \, du_i \, dv_j$. This is represented in the integral by the absolute value of the Jacobian determinant associated with the parameterization: $\|\overrightarrow{\partial_u P} \times \overrightarrow{\partial_v P}\|$.

4.4.1 The divergence theorem

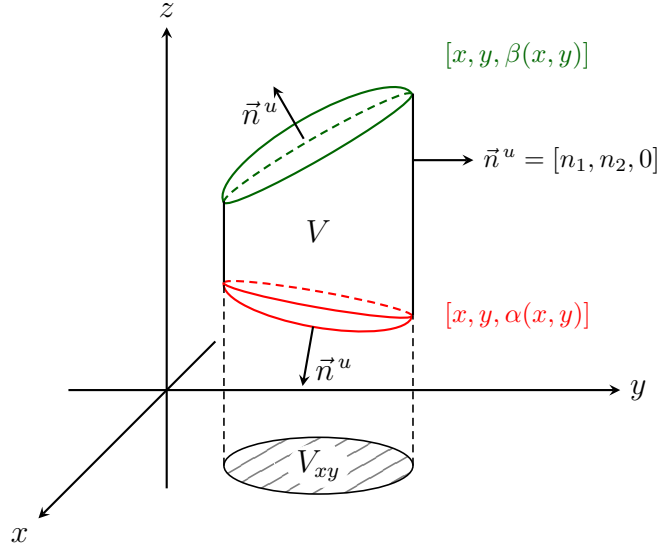


Figure 14: Proof of the divergence theorem. The normal region V is projected onto the XY -plane, with projection V_{xy} . The upper and lower boundaries of V are represented by a parametrization.

4.6.0 The corkscrew rule

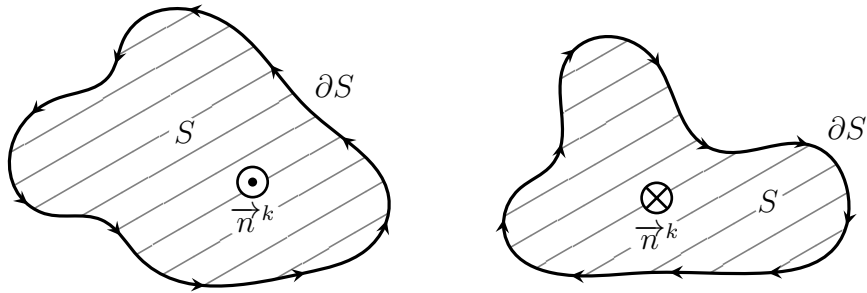


Figure 15: The unit vector along the surface normal, \vec{n}^k , is oriented such that its direction agrees with the orientation of ∂S according to the corkscrew rule (or right-hand rule).

4.6.1 Stokes theorem

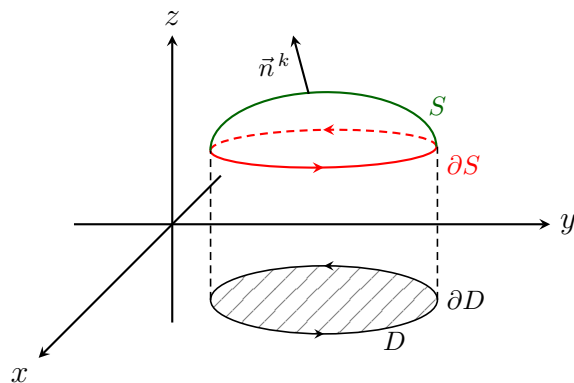


Figure 16: Proof Stokes' theorem. S is a smooth surface that can be projected onto the XY -plane, with projection D .

5.1 Inverse function

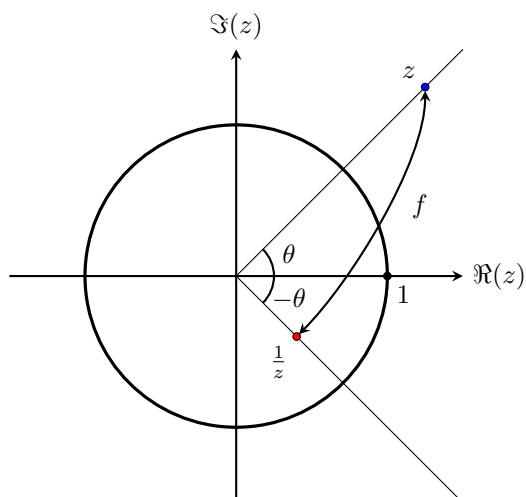


Figure 17:

5.1 Complex function

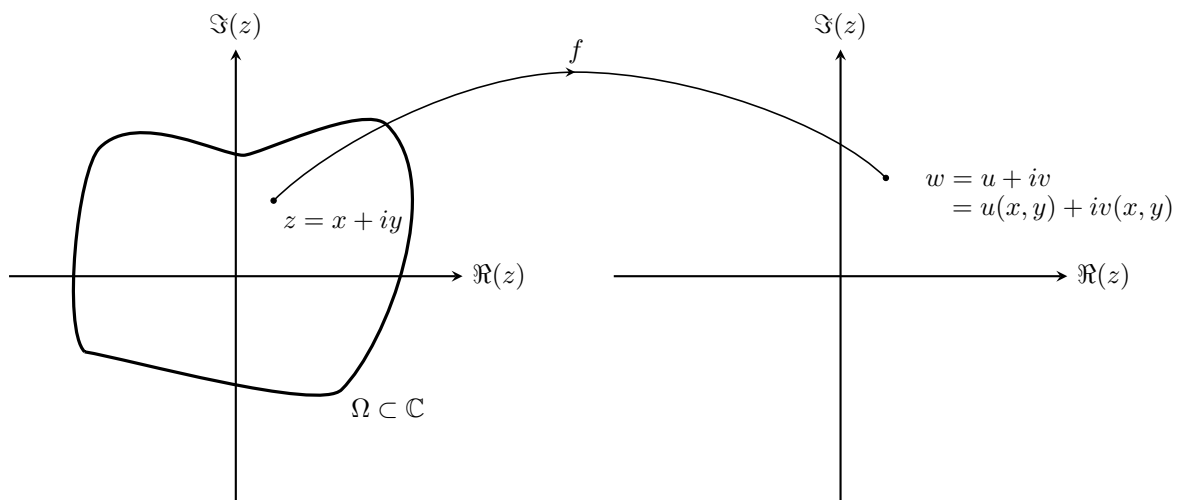


Figure 18:

5.2 Complex line integral

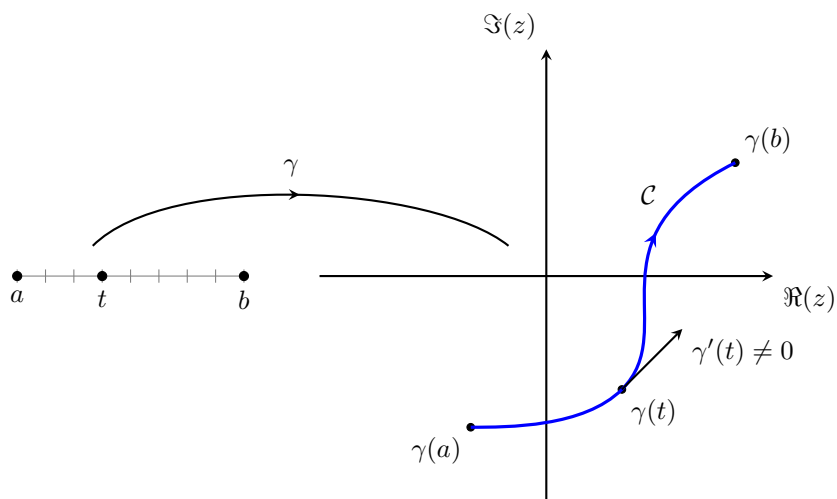


Figure 19:

6.2.1 Complex derivative

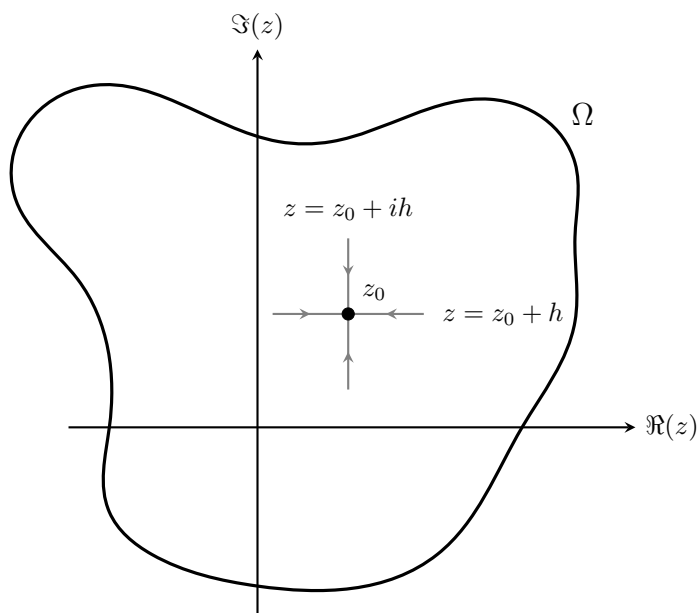


Figure 20: The complex derivative in a point $z_0 = x_0 + iy_0$ for a complex function is: $f'(z_0) = \lim_{h \rightarrow 0} \frac{f(z_0+h) - f(z_0)}{h}$. For $f'(z_0)$ to exist, this limit must be the same regardless of the direction in which $h \rightarrow 0$. In the figure, the limit is approached along the real and imaginary axes; equating the results of both approaches yields the Cauchy–Riemann conditions.

6.3 Cauchy Goursat theorem for multiply connected domains

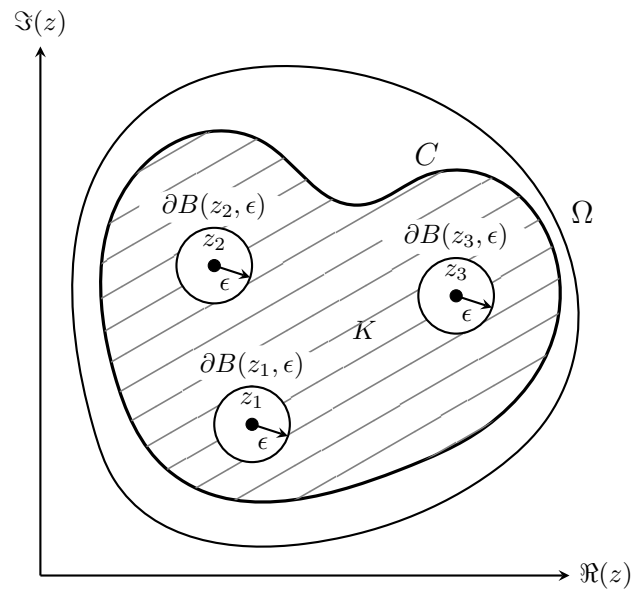


Figure 21:

6.3 Contour non simply connected

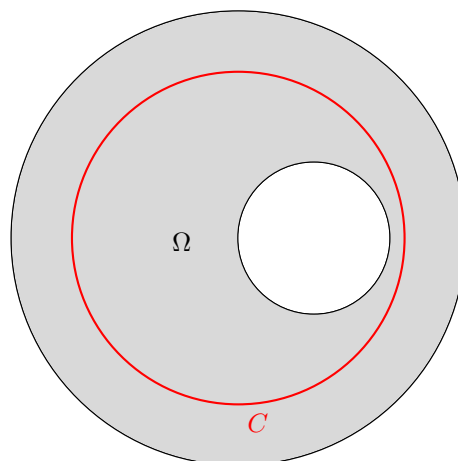


Figure 22:

6.3 Contour simply connected

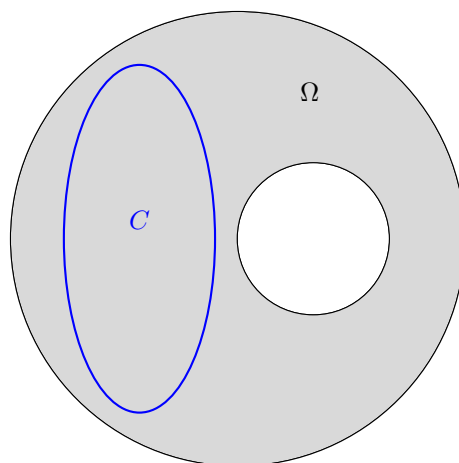


Figure 23:

6.3.3 Proof integral formula Cauchy

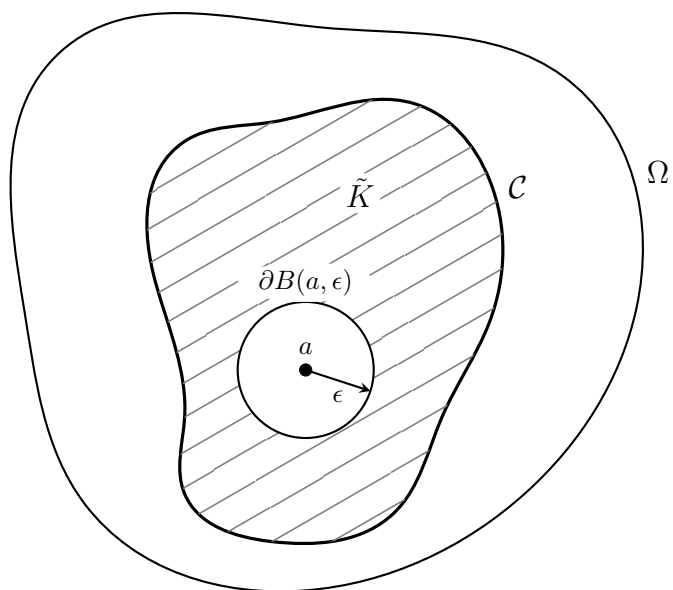


Figure 24: \mathcal{C} is a bounded contour in Ω which encloses a compact set K lying completely within Ω . For a point $a \in \mathcal{C} \setminus K$, we parametrize the circle $\partial B(a, \epsilon)$, which lies entirely in the interior of \mathcal{C} .

7.2.4 Theorem convergence regions positive and negative power series

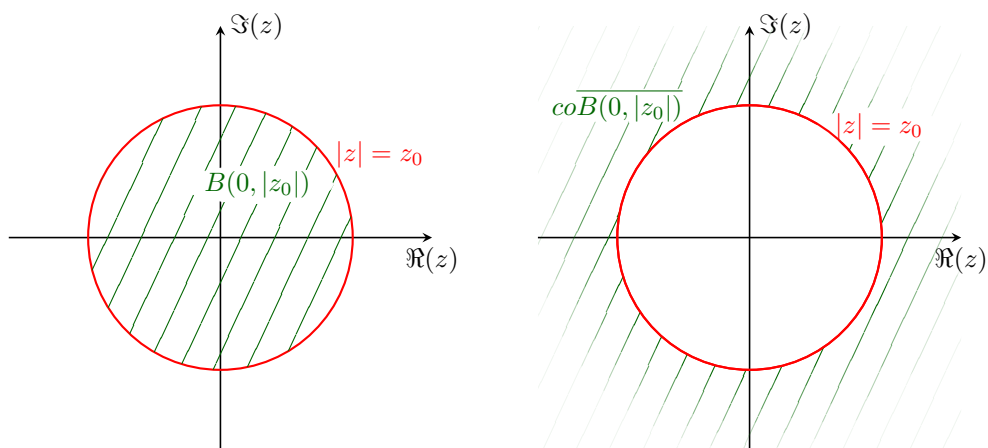


Figure 25: (Left) Region of convergence of a positive power series. (Right) Region of convergence of a negative power series.

8.2.1 Proof theorem Laurent series

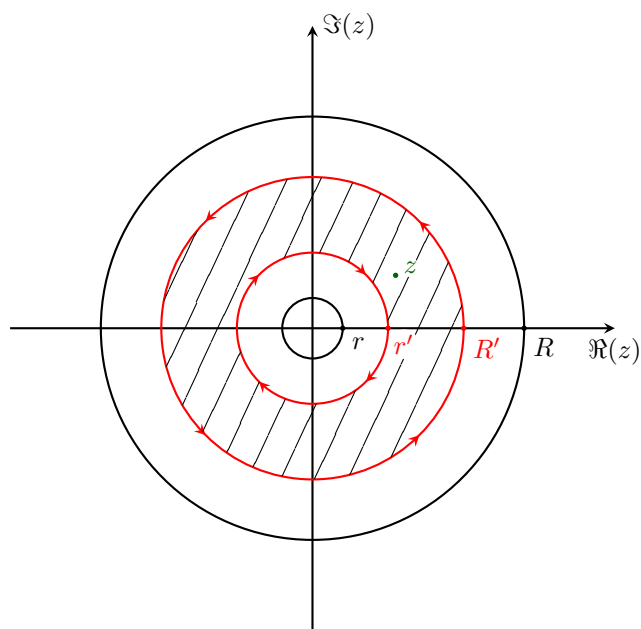


Figure 26: The region of convergence of the Laurent series is the annular region $B(0, R) \setminus \overline{B(0, r)}$. For every point z , it is possible to find R' and r' such that $0 < r < r' < |z| < R' < R$.

8.5.6 Residue theorem for region with multiple singularities

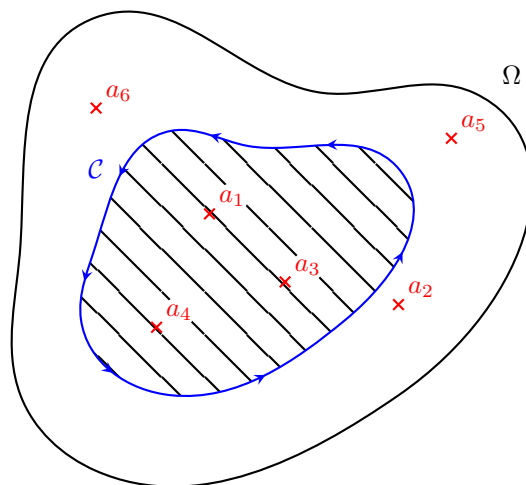


Figure 27: The contour \mathcal{C} passes through none of the singularities a_i of the complex function f and encloses a compact set that lies entirely within Ω . \mathcal{C} contains a finite number of singularities of f .

9.3 Estimation lemmas

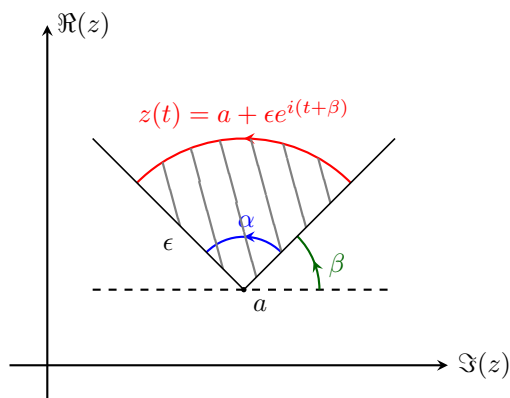


Figure 28: Small limit theorem: The circular arc C_ε^t with center a , radius $\varepsilon > 0$, and central angle α can be described by the parametric equation $z(t) = a + \varepsilon e^{i(t+\beta)}$, $t : 0 \rightarrow \alpha$.

9.5 Summation of series

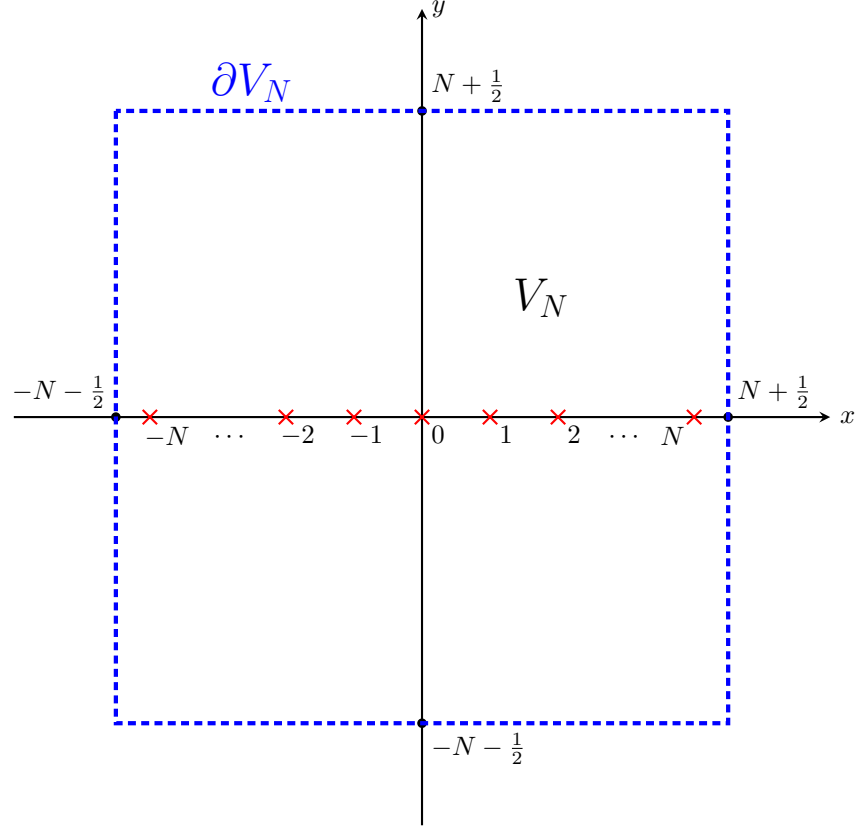


Figure 29: The function $g(z) = \cot(\pi z)$ has simple poles at $z = 0, \pm 1, \pm 2, \dots$. If we consider the square V_N with center at the origin and side length $2N + 1$, where $N \in \mathbb{N}$, then we can compute the contour integral over ∂V_N^+ using the residue theorem.